Advances in Applied Mathematics and Mechanics
Adv. Appl. Math. Mech., Vol. **9**, No. 4, pp. 887-903

DOI: 10.4208/aamm.2016.m1423
August 2017

A Hybrid Dynamic Mesh Generation Method for Multi-Block Structured Grid

Hao Chen, Zhiliang Lu* and Tongqing Guo

College of Aerospace Engineering, Nanjing University of Aeronautics and Astronautics, Nanjing, Jiangsu 210016, China

Received 25 January 2016; Accepted (in revised version) 18 July 2016

Abstract. In this paper, a hybrid dynamic mesh generation method for multi-block structured grid is presented based on inverse distance weighting (IDW) interpolation and transfinite interpolation (TFI). The major advantage of the algorithm is that it maintains the effectiveness of TFI, while possessing the ability to deal with multi-block structured grid from the IDW method. In this approach, dynamic mesh generation is made in two steps. At first, all domain vertexes with known deformation are selected as sample points and IDW interpolation is applied to get the grid deformation on domain edges. Then, an arc-length-based TFI is employed to efficiently calculate the grid deformation on block faces and inside each block. The present approach can be well applied to both two-dimensional (2D) and three-dimensional (3D) problems. The proposed method has been well-validated by several test cases. Numerical results show that dynamic meshes with high quality can be generated in an accurate and efficient manner.

AMS subject classifications: 65Z05

Key words: Multi-block structured grid, mesh deformation, inverse distance weighting, transfinite interpolation.

1 Introduction

Unsteady flow calculations for problems with deformable boundaries, such as those in aeroelastic simulations, require a fast and robust method for regeneration of the computational grid in each time step. For generation of a single-block dynamic mesh, transfinite interpolation [1–5] (TFI) method with an algebraic interpolation is frequently used. Its efficiency is still very high when the grid size is large. However, TFI is very difficult to be applied for a complex geometry when a multi-block structured grid is used. This

*Corresponding author.
Email: luzl@nuaa.edu.cn (Z. L. Lu)

 ©2017 Global Science Press

https://doi.org/10.4208/aamm.2016.m1423 Published online by Cambridge University Press

is because mesh points on block edges are irregularly distributed when the mesh is deformed. Therefore, the main problem is the computation of the displacement of edges in a multi-block grid.

Point-by-point methods do not rely on connectivity information as they determine the displacement of each mesh point based on its relative position with respect to the domain boundary. Inverse distance weighting (IDW) interpolation [6–8] is an explicit interpolation technique, which computes the interpolation function as a weighted average of the known boundary node displacements. In contrast to radial basis function (RBF) interpolation [9–11], it does not require solving a system of equations for deforming the volume mesh. The IDW interpolation is found to be faster than RBF [12]. However, in terms of computational effort, it is still expensive, especially in the case where the number of interior and boundary nodes is large. For example, a mesh with approximately 3 million nodes, of which 130,000 are boundary nodes, has a deformation time of 2 hours in serial mode [13]. Luke et al. [14] used a tree-code optimization to increase the efficiency of IDW for large scale meshes. However, this method is fairly complicated and there are several input parameters for the users to tune according to different geometries. Moreover, for IDW interpolation, the distance-decay effect can be influenced by a power parameter c [15]. Large values of c result in an interpolation that is influenced mainly by the closest points. On the other hand, lower values of c result in smooth interpolations where the solution at a point is influenced by more distant points. Witteveen [16] proposed to use different values for the power parameter c for rotation and translation and spatially non-uniform power parameter distributions based on data density have been used in adaptive IDW [17].

In order to solve aforementioned problems, a novel mesh deformation method for multi-block structured grid based on inverse distance weighting interpolation and transfinite interpolation is presented in this paper. In this approach, only the domain vertexes with known displacements are selected as sample points so as to improve the efficiency while the quality of mesh deformation is only affected very little and IDW interpolation is merely utilized to generate the dynamic mesh on domain edges, decreasing the impact of the power parameter on the dynamic mesh quality. Then, an arc-length-based TFI is adopted to generate structured mesh on block faces and within each block. The major advantage of the proposed method is that it maintains the effectiveness of TFI, while possessing the ability to handle multi-block structured grid from the IDW method. As compared with the traditional IDW method, the hybrid method can greatly improve the efficiency of grid generation and the generated mesh usually has good quality. Furthermore, the users don't need to spend much time on adjusting affected parameters according to different geometries. This is because the only affected parameter, power parameter, has little influence on the mesh quality.

The present hybrid method is firstly applied to the dynamic mesh generation for two two-dimensional (2D) and one three-dimensional (3D) problems with different complexity. Then numerical simulation of a 2D unsteady flow is conducted. The results demonstrate that dynamic meshes for all test cases can be generated in an accurate and efficient

https://doi.org/10.4208/aamm.2016.m1423 Published online by Cambridge University Press

manner.

2 Mesh deformation on domain edges by IDW interpolation

2.1 IDW interpolation

Inverse distance weighting interpolation is an explicit method for multivariate interpolation of scattered data points. It was first introduced in 1968 by Shepard in the frame work of geographical information systems [18]. The interpolation surface $w(\mathbf{x})$ through n data samples $\mathbf{v}=\{v_1,\cdots,v_n\}$ of the exact function $u(\mathbf{x})$ with $v_i\equiv u(\mathbf{x}_i)$ is given in inverse distance weighting by

$$w(\mathbf{x})=\frac{\sum_{i=1}^{n} v_i\phi(r_i)}{\sum_{i=1}^{n}\phi(r_i)} \tag{2.1}$$

with weighting function

$$\phi(r)=r^{-c}, \tag{2.2}$$

where $r_i=\|\mathbf{x}-\mathbf{x}_i\|\geq 0$ is the Euclidean distance between $\mathbf{x}$ and data point $\mathbf{x}_i$ and c is a power parameter.

2.2 The impact of the number of sample points on the quality of mesh deformation

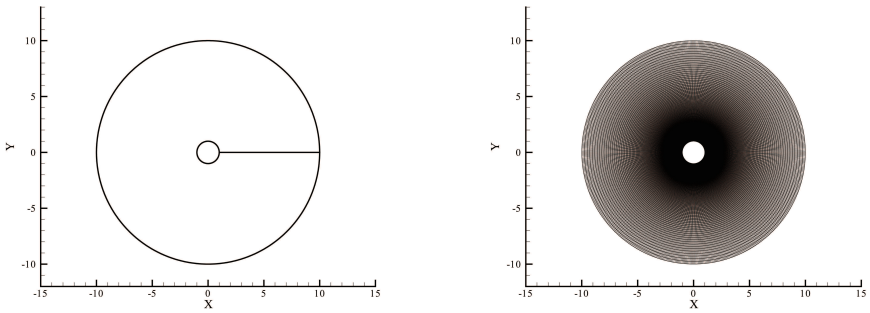
Conventionally, all the grid points with known displacements are selected as sample points and the computational efficiency is very low in the case of a large number of sample points. Firstly, the impact of the number of sample points on the quality of mesh deformation by IDW interpolation is discussed via a simple example. A single-block structured O-type mesh is generated, see Fig. 1, 601×200 in the wrap-around and outward directions. In this case, the internal circle surface is subject to a given displacement of translation $\Delta x=1.0$, while the outer boundary is fixed. When all the grid points with known displacements are selected as sample points, there are 1,200 points. Now two test cases, namely 120 sample points and 12 sample points evenly distributed on the boundary as shown in Fig. 2 (red points), are adopted to research its influence on the dynamic mesh quality by IDW interpolation.

There are many mesh checking methods, such as angle skewness, aspect ratio, determinant and so on. In this paper, angle skewness is used as a measure of the mesh quality. The angle skewness is computed as follows [19]:

$$Q=1.0-\max\left(\frac{\theta_{Max}-\theta_A}{180-\theta_A},\frac{\theta_A-\theta_{Min}}{\theta_A}\right), \tag{2.3}$$

where θ_{Max} and θ_{Min} are the largest included angle and the smallest one respectively, and θ_A is the average included angle of the checked cell. For example, θ_A equals to 90 degrees

https://doi.org/10.4208/aamm.2016.m1423 Published online by Cambridge University Press



(a) (b)

Figure 1: Initial O-type mesh.



(a) (b)

Figure 2: Sample points distribution: 120 points on the left and 12 points on the right.

for a quadrangle cell. A skewness of 1 indicates a perfect cell, and 0 indicates that the cell is degenerate. All the CPU times are taken from a single 3.10GHz Intel processor.

Table 1 shows the average quality of mesh deformation by using different number of sample points with power parameter $c = 5.0$. When the number of sample points decrease to one percent, the quality of mesh deformation is only affected very little while the efficiency is raised greatly.

To demonstrate the generality, a O-type mesh of NACA0012 is generated, see Fig. 3, 406×58 in the wrap-around and outward directions. In this case, the airfoil rotates 5 degrees about its quarter-chord point. Table 2 shows the dynamic mesh quality by us-

Table 1: The influence of different number of sample points by IDW.

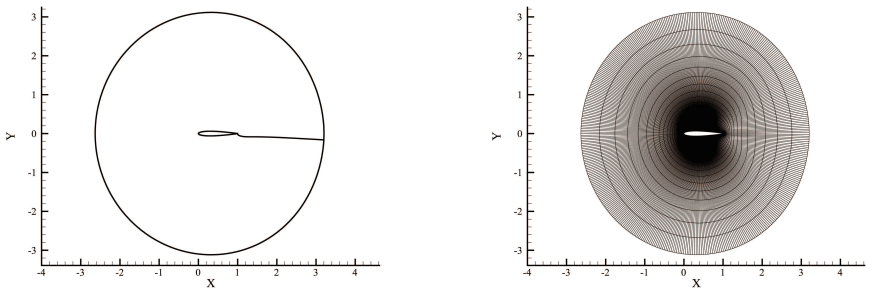
	the number of sample points		
	1,200	120	12
Average mesh quality	0.979	0.979	0.978
CPU-time/s	2.558	0.265	0.031

https://doi.org/10.4208/aamm.2016.m1423 Published online by Cambridge University Press

Table 2: The influence of different number of sample points by IDW.

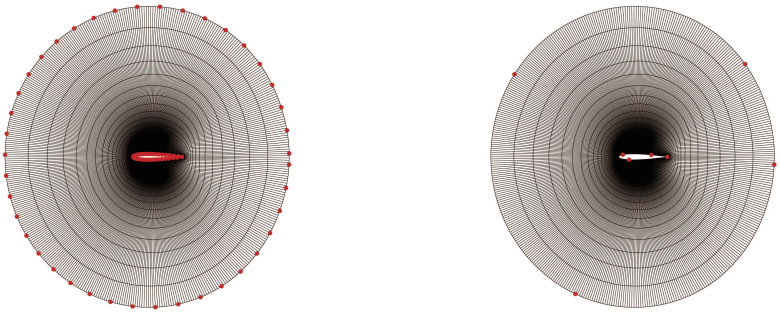
	the number of sample points		
	810	82	8
Average mesh quality	0.975	0.975	0.975
CPU-time/s	1.186	0.125	0.016

ing different number of sample points, as shown in Fig. 4. However, it's important to note that the number and distribution of sample points must be reasonable to reflect the deformation characteristics. Otherwise, the interpolation precision can't be ensured.



(a) (b)

Figure 3: Initial O-type mesh.



(a) (b)

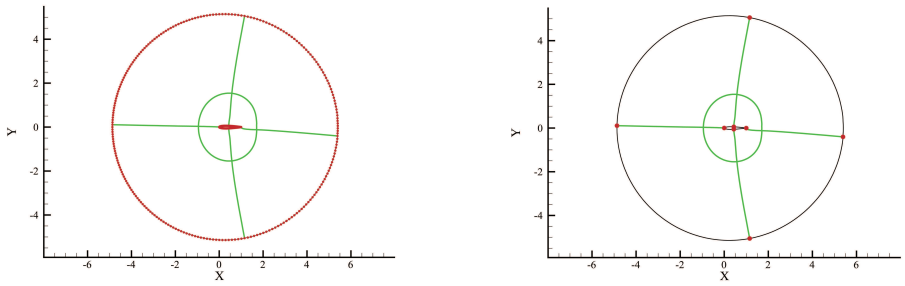
Figure 4: Sample points distribution: 82 points on the left and 8 points on the right.

2.3 Mesh deformation on domain edges

2.3.1 Choice of sample points for IDW interpolation

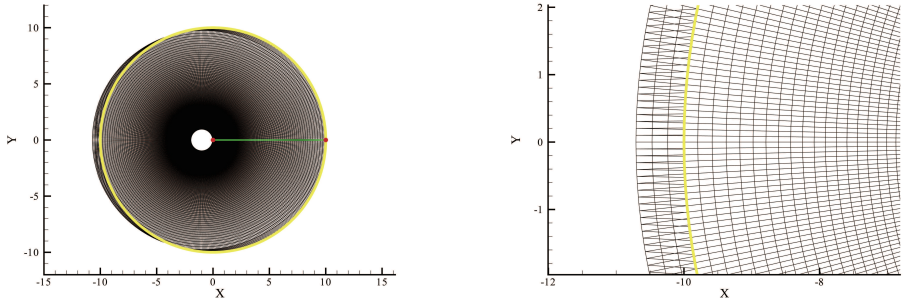
From what has been discussed above, it is necessary to reduce the number of sample points for IDW interpolation. In this paper, we proposed that only the domain ver-

https://doi.org/10.4208/aamm.2016.m1423 Published online by Cambridge University Press



(a) (b)

Figure 5: Selection of sample points: 492 points on the left and 8 points on the right.



(a) (b)

Figure 6: Deformed mesh after IDW interpolation, 2 sample points.

texes with known displacements are selected as sample points. This can greatly speed up the process of mesh deformation. An example is shown in Fig. 5. When all the grid points with known displacements (red points) are selected as sample points, there are 492 points. On the other hand, when only the domain vertexes with known displacements are selected as sample points, there are only 8 sample points.

However, this way of selecting sample points is not suitable for the traditional IDW method. This is because when there are only a small number of sample points and the distribution is unreasonable, interpolation precision is not accurate enough. Take Fig. 1 as an example, a single-block grid, there are just 2 sample points and the mesh crosses over after the translation, see Fig. 6, the interior nodes have exceed the far field boundary (yellow curves). Although it's possible to divide more blocks to increase the number of sample points, it is inconvenient. To overcome the disadvantage, in this paper only domain edges are based on IDW interpolation and TFI is adopted to generate structured mesh on block faces and within each block. Several numerical cases in Section 4 can be used to prove its feasibility.

https://doi.org/10.4208/aamm.2016.m1423 Published online by Cambridge University Press

2.3.2 Mesh generation on domain edges

The blue point in Fig. 7 is a point on one of green edges whose displacements are unknown. Now set all domain vertexes with known displacements (red points) as sample points and blue point as interpolative dot, the displacement of blue point can be calculated by all red points easily with IDW interpolation. Similarly, other grid points on this edge and other edges can be worked out one by one. As shown in Fig. 8, an airfoil rotates 45 degrees about its quarter-chord point, deformation of all domain edges (green curves) can be obtained with IDW interpolation. Since IDW is merely utilized to generate the dynamic mesh on domain edges with just a few sample points, the power parameter has little influence on the mesh quality.

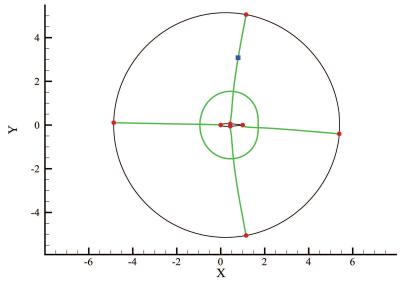


Figure 7: Generation of mesh deformation on domain edges.

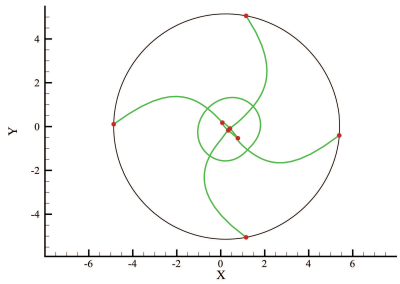


Figure 8: Deformed domain edges after IDW interpolation.

3 Mesh deformation on block faces and within each block by TFI interpolation

After computing the displacement of mesh points on all domain edges by IDW interpolation method, the displacement of grid points in the interior of faces is computed by a 2-D TFI method. Then, a 3-D TFI method is further used to compute the displacement

https://doi.org/10.4208/aamm.2016.m1423 Published online by Cambridge University Press

of mesh points in the interior of each block. This method can effectively preserve the original character of the mesh.

By using the Boolean sum of interpolation functions, a 3-D TFI can be written as

$$\Delta x_{i,j,k}=U+V+W-UV-VW-UW+UVW, \tag{3.1}$$

where the grid deformation is defined as

$$\Delta x_{i,j,k}=[\Delta x_{i,j,k},\Delta y_{i,j,k},\Delta z_{i,j,k}]. \tag{3.2}$$

The univariate products and the tensor products are evaluated as follows:

$$U=(1-\alpha_{i,j,k})\Delta x_{1,j,k}+\alpha_{i,j,k}\Delta x_{i\max,j,k}, \tag{3.3a}$$

$$V=(1-\beta_{i,j,k})\Delta x_{i,1,k}+\beta_{i,j,k}\Delta x_{i,j\max,k}, \tag{3.3b}$$

$$W=(1-\gamma_{i,j,k})\Delta x_{i,j,1}+\gamma_{i,j,k}\Delta x_{i,j,k\max}, \tag{3.3c}$$

and

$$\begin{aligned}UV=&(1-\alpha_{i,j,k})(1-\beta_{i,j,k})\Delta x_{1,1,k}+\alpha_{i,j,k}(1-\beta_{i,j,k})\Delta x_{i\max,1,k}\\&+(1-\alpha_{i,j,k})\beta_{i,j,k}\Delta x_{1,j\max,k}+\alpha_{i,j,k}\beta_{i,j,k}\Delta x_{i\max,j\max,k},\end{aligned} \tag{3.4a}$$

$$\begin{aligned}VW=&(1-\beta_{i,j,k})(1-\gamma_{i,j,k})\Delta x_{i,1,1}+\beta_{i,j,k}(1-\gamma_{i,j,k})\Delta x_{i,j\max,1}\\&+(1-\beta_{i,j,k})\gamma_{i,j,k}\Delta x_{i,1,k\max}+\beta_{i,j,k}\gamma_{i,j,k}\Delta x_{i,j\max,k\max},\end{aligned} \tag{3.4b}$$

$$\begin{aligned}UW=&(1-\alpha_{i,j,k})(1-\gamma_{i,j,k})\Delta x_{1,j,1}+\alpha_{i,j,k}(1-\gamma_{i,j,k})\Delta x_{i\max,j,1}\\&+(1-\alpha_{i,j,k})\gamma_{i,j,k}\Delta x_{1,j,k\max}+\alpha_{i,j,k}\gamma_{i,j,k}\Delta x_{i\max,j,k\max},\end{aligned} \tag{3.4c}$$

$$\begin{aligned}UVW=&(1-\alpha_{i,j,k})(1-\beta_{i,j,k})(1-\gamma_{i,j,k})\Delta x_{1,1,1}+\alpha_{i,j,k}(1-\beta_{i,j,k})(1-\gamma_{i,j,k})\Delta x_{i\max,1,1}\\&+(1-\alpha_{i,j,k})\beta_{i,j,k}(1-\gamma_{i,j,k})\Delta x_{1,j\max,1}+(1-\alpha_{i,j,k})(1-\beta_{i,j,k})\gamma_{i,j,k}\Delta x_{1,1,k\max}\\&+\alpha_{i,j,k}\beta_{i,j,k}(1-\gamma_{i,j,k})\Delta x_{i\max,j\max,1}+\alpha_{i,j,k}(1-\beta_{i,j,k})\gamma_{i,j,k}\Delta x_{i\max,1,k\max}\\&+(1-\alpha_{i,j,k})\beta_{i,j,k}\gamma_{i,j,k}\Delta x_{1,j\max,k\max}+\alpha_{i,j,k}\beta_{i,j,k}\gamma_{i,j,k}\Delta x_{i\max,j\max,k\max}.\end{aligned} \tag{3.4d}$$

In order to maintain the grid distribution laws of the initial grid, an arc-length-based TFI method [20] is applied in this work. The arc-length-based control functions along i, j, k directions are defined as

$$\alpha_{1,j,k}=0, \qquad \beta_{i,1,k}=0, \qquad \gamma_{i,j,1}=0, \tag{3.5a}$$

$$\alpha_{i,j,k}=\frac{\sum_{m=2}^{i}\left\|x_{m,j,k}-x_{m-1,j,k}\right\|}{\sum_{m=2}^{i\max}\left\|x_{m,j,k}-x_{m-1,j,k}\right\|}, \quad \beta_{i,j,k}=\frac{\sum_{m=2}^{j}\left\|x_{i,m,k}-x_{i,m-1,k}\right\|}{\sum_{m=2}^{j\max}\left\|x_{i,m,k}-x_{i,m-1,k}\right\|}, \quad \gamma_{i,j,k}=\frac{\sum_{m=2}^{k}\left\|x_{i,j,m}-x_{i,j,m-1}\right\|}{\sum_{m=2}^{k\max}\left\|x_{i,j,m}-x_{i,j,m-1}\right\|}. \tag{3.5b}$$

Take Fig. 9 as an example, for any structured face, displacements of point $P(i,j)$ are computed by 8 points. For each single structured block, displacements of point $P(i,j,k)$ are calculated by 26 points in the block as shown in Fig. 10. More details about TFI can be found in [21]. Fig. 11 shows the overall deformed mesh of NACA0012 rotating 45 degrees by using the IDW-TFI method. The mesh smoothness at the block interfaces maintains good.

https://doi.org/10.4208/aamm.2016.m1423 Published online by Cambridge University Press

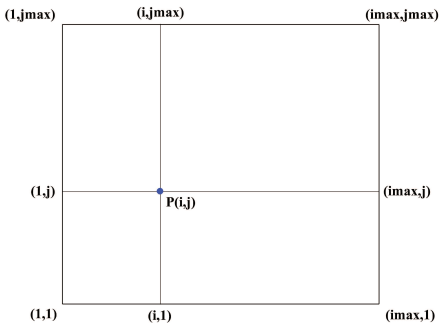


Figure 9: 2-D TFI sketch.

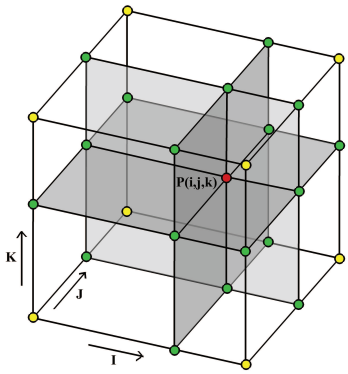


Figure 10: 3-D TFI sketch.

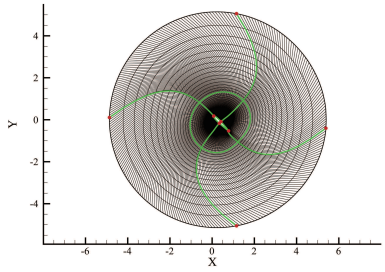


Figure 11: Deformed mesh of NACA0012 by using the IDW-TFI method.

4 Numerical cases

The present IDW-TFI hybrid method has been applied to two 2D and one 3D mesh deformation problems with different complexity. After that, simulation of unsteady viscous

https://doi.org/10.4208/aamm.2016.m1423 Published online by Cambridge University Press

flows around a moving airfoil is performed to show the accuracy of this method. The dynamic meshes for the above test cases have been generated in an accurate and efficient manner.

4.1 Test case 1: circle translation

Take the previous circle translation case in Section 2.2 as an example, Table 3 shows the average mesh quality with different number of sample points by using the present IDW-TFI method.

Fig. 12 shows the deformed mesh. In contrary to Fig. 6, the interpolation precision of IDW-TFI is enough when there are just 2 sample points. As compared with the traditional IDW method, see Table 1, the present IDW-TFI method can greatly improve the efficiency of dynamic mesh generation while the quality of mesh deformation is only decreased by 0.002.

In the present IDW-TFI hybrid method, if we use RBF to replace IDW, namely RBF-TFI, when there are too many sample points, IDW-TFI is faster than RBF-TFI. Table 4 shows the mesh quality and CPU-time by RBF-TFI and IDW-TFI based on 1,200 sample points.

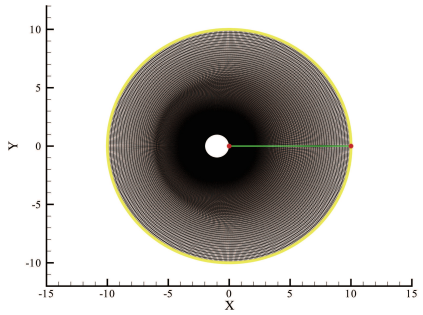


Figure 12: Deformed mesh by IDW-TFI, 2 sample points.

Table 3: The influence of different number of sample points by IDW-TFI.

	the number of sample points	
	1,200	2
Average mesh quality	0.979	0.977
CPU-time/s	0.036	0.002

Table 4: Average mesh quality and CPU-time by RBF-TFI and IDW-TFI.

	RBF-TFI	IDW-TFI
Average mesh quality	0.973	0.979
CPU-time/s	22.761	0.036

https://doi.org/10.4208/aamm.2016.m1423 Published online by Cambridge University Press

4.2 Test case 2: aerodynamic shape optimization

Mesh deformation is often used in aerodynamic shape optimization [22,23]. For each new value of design variables, a new mesh must be obtained. In this case, NACA0012 airfoil is the initial shape and NACA0020 airfoil is the optimized shape. NACA0020 airfoil is used to deform NACA0012 airfoil suddenly without changing the characteristics of the initial mesh. Fig. 13 shows the initial shape and deformed shape. Fig. 14 shows an initial 8 blocks of *O*-type mesh of NACA0012, and the number of grid cells is 26,215.

In Section 2.3.1, we proposed that only the domain vertexes with known displacements are selected as sample points. However, this way of selecting sample points is not suitable for the single IDW method. Fig. 15 shows the deformed mesh by IDW with 8 sample points. The interpolation precision is not accurate near airfoil surface (red curves).

Both the traditional IDW method with whole known displacements points as sample points and present IDW-TFI hybrid method are applied for the new mesh generation.

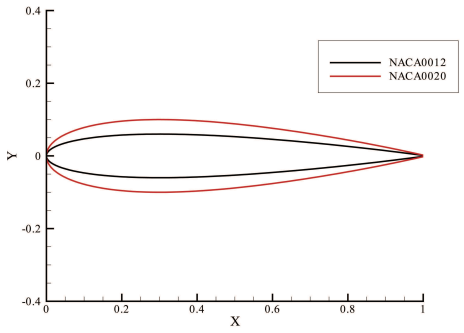
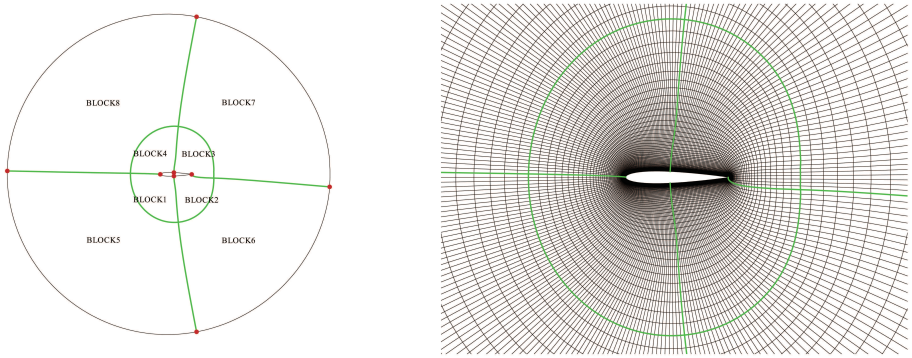


Figure 13: NACA0012 airfoil and NACA0020 airfoil.



(a) (b)

Figure 14: Initial mesh of NACA0012: (a) Topology. (b) Close-up view.

https://doi.org/10.4208/aamm.2016.m1423 Published online by Cambridge University Press

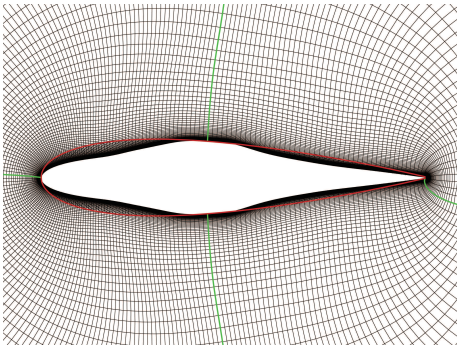


Figure 15: Deformed mesh of NACA0020 by IDW, 8 sample points.

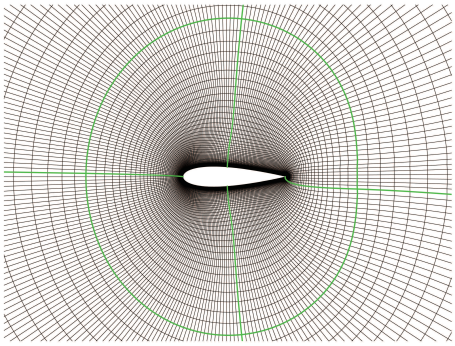


Figure 16: Deformed mesh of NACA0020 by using the IDW-TFI method.

Results for the average mesh quality with three different power parameter values are given in Table 5. The mesh quality of IDW-TFI is comparable with IDW. However, the IDW power parameter has greater influence on the mesh quality. For IDW-TFI, only domain edges are based on IDW interpolation with just a few sample points. So it can reduce the influence of the power parameter on the mesh quality. For power parameter $c=5.0$, Fig. 16 shows the deformed mesh by using the IDW-TFI method. The CPU-time required by IDW is 0.234s, and it is only 0.078s needed by the present hybrid method. On the other hand, the average mesh quality of RBF-TFI is 0.858 which is lower than IDW-TFI. The CPU-time cost by RBF-TFI is almost the same as IDW-TFI because there are only 8 sample points in this case.

4.3 Test case 3: high-aspect-ratio wing

Test case 3 involves a high-aspect-ratio wing model. In this case, the wing undergoes a vertical bending deformation and the maximum deformation at the wingtip is 5.0 meters. Fig. 17 shows the initial and deformed configurations. The topology is displayed in Fig. 18. The number of grid blocks is 4, and the number of grid cells is 899,542.

https://doi.org/10.4208/aamm.2016.m1423 Published online by Cambridge University Press

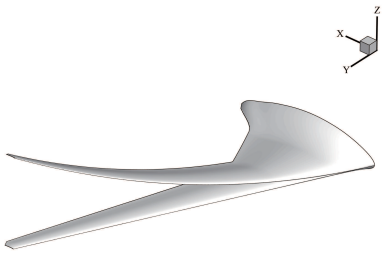


Figure 17: Initial and deformed configurations of a 3D wing.

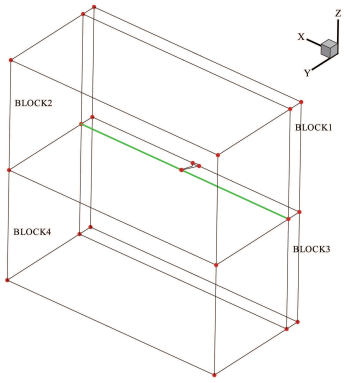


Figure 18: Topology of a 3D wing.

For a 3-D dynamic re-meshing problem, the traditional IDW method will select all block face points with known displacements as sample points, which can be so large that unbearable CPU-time is required. In contrast, the present IDW-TFI method takes the domain vertexes with known displacements as sample points. As shown in Fig. 18, there are only 22 sample points (red points) for this case and just two green domain edges are based on IDW interpolation. For power parameter $c=2.0$, IDW has a deformation time of half an hour, and it is only 1.264s needed by IDW-TFI which is about 0.07% of the former. This indicates that the present method is much more efficient. Fig. 19 shows the deformed mesh by using the IDW-TFI method.

Table 5: Average mesh quality with different power parameter values.

Power parameter	Average mesh quality	
	IDW	IDW-TFI
2.0	0.856	0.917
3.0	0.913	0.915
5.0	0.919	0.914

https://doi.org/10.4208/aamm.2016.m1423 Published online by Cambridge University Press

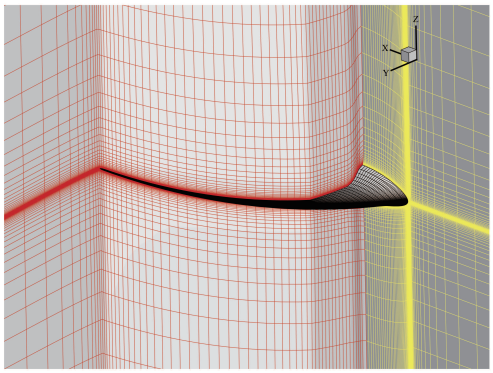


Figure 19: Deformed mesh of a 3D wing by using the IDW-TFI method.

Table 6: Average mesh quality with different power parameter values.

Power parameter	Average mesh quality	
	IDW	IDW-TFI
2.0	0.747	0.759
3.0	0.756	0.759
5.0	0.759	0.759

Table 6 shows the average mesh quality of the deformed mesh with three different power parameter values. The initial mesh quality is 0.778. It can be seen that the IDW-TFI power parameter has little influence on the mesh quality and the average mesh quality dropped by less than 2.5% as compared to the undeformed wing. It proves that the present hybrid mesh deformation method has enough robustness and can be applied to wings with large deformations. In this case, numerical experiments showed that there is no significant difference on the mesh quality and CPU-time between IDW-TFI and RBF-TFI.

4.4 Test case 4: unsteady flow around airfoil

The fourth test case is numerical simulation of an unsteady flow associated with mesh deformation. The number of grid cells is 17,395 and the distance of the first grid line off surface is about 10^{-5} chord length. In this case, a NACA0012 airfoil is forced to pitch around the quarter chord with a reduced frequency of 0.0808. The pitching motion is given as follows:

$$\alpha = 2.89^\circ + 2.41^\circ \sin(2kt), \tag{4.1}$$

where α is the angle of attack, k is the reduced frequency, t is the time. The Mach number M_a in this simulation is set as 0.60. The lift force coefficient calculated by NS equations is shown in Fig. 20 along with corresponding experimental data [24] and the reference data

https://doi.org/10.4208/aamm.2016.m1423 Published online by Cambridge University Press

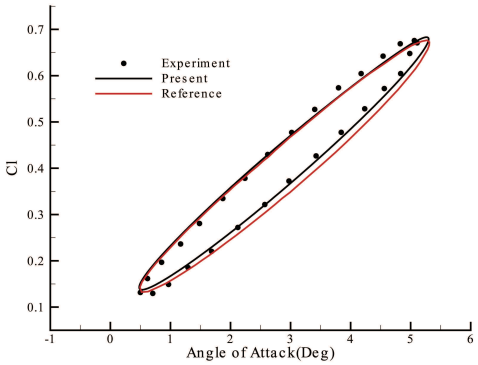


Figure 20: Unsteady Cl Variation with the Angle of Attack for NACA0012 airfoil.

calculated by Li et al. [25]. Overall, the present numerical results have a good agreement with the experimental data and are more accurate than the reference data. This implies that the present hybrid method can be effectively applied to solve the real complicated flow problems.

5 Conclusions

By combining IDW and TFI, a novel mesh deformation method is proposed in this work for generation of dynamic multi-block structured grids. The major advantage of this method is that it maintains the effectiveness of TFI method, while possessing the ability to handle multi-block structured grid. As compared with the traditional IDW method, the present method can greatly improve the efficiency of grid generation and the generated mesh usually has good quality, which is less influenced by the power parameter. The power parameter $c = 2.0$ is commonly chosen because it yields satisfactory results with the least computational effort. By using the present method, dynamic mesh with millions of grid cells can be efficiently generated within several seconds while the traditional IDW method may take half an hour.

Acknowledgements

This work was supported by the National Natural Science Foundation of China (Grant No. 11372135), the National Basic Research Program of China ("973" Project) (Grant No. 2014CB046200) and the Priority Academic Program Development of Jiangsu Higher Education Institutions.

https://doi.org/10.4208/aamm.2016.m1423 Published online by Cambridge University Press

References

[1] A. L. GAITONDE AND S. P. FIDDES, *A moving mesh system for the calculation of unsteady flows,* AIAA Paper 93-0461, January 1993.

[2] J. REUTHER, A. JAMESON, J. FARMER, L. MARTINELLI AND D. SAUNDERS, *Aerodynamics shape optimization of complex aircraft configurations via an adjoint formulation,* AIAA Paper 96-0094, January 1996.

[3] C. BYUN AND G. P. GURUSWAMY, *A parallel, multi-block, moving grid method for aeroelastic applications on full aircraft,* AIAA Paper 98-4782, September 1998.

[4] C. B. ALLEN, *An algebraic grid motion technique for large deformations*, J. Aerospace Eng., 216(1) (2002), pp. 51–58.

[5] Z. L. LU, *Generation of dynamic grids and computation of unsteady transonic flows around assemblies,* China J. Aeron., 14 (2001), pp. 1–5.

[6] P. M. BARTIER AND C. P. KELLER, *Multivariate interpolation to incorporate thematic surface data using inverse distance weighting,* Comput. Geosci., 22(7) (1996), pp. 795–799.

[7] G. PAPARI AND N. PETKOV, *Reduced inverse distance weighting interpolation for painterly rendering,* Comput. Anal. Images Patterns, (2009), pp. 509–516.

[8] Y. ZHAO AND AHMED FORHAD, *A general method for simulation of fluid flows with moving and compliant boundaries on unstructured grids,* Comput. Methods Appl. Mech. Eng., 192 (2003), pp. 4439–4466.

[9] A. B. ECKERT AND H. WENLAND, *Multivariate interpolation for fluid-structure-interaction problems using radial basis functions,* Aerospace Sci. Technol., 5 (2001), pp. 125–134.

[10] A. DE BOER, M. S. VAN DER SCHOOT AND H. BIJL, *Mesh deformation based on radial basis function interpolation,* Comput. Structures, 85 (2007), pp. 784–795.

[11] T. C. S RENDALL AND C. B. ALLEN, *Unified fluid-structure interpolation and mesh motion using radial basis functions,* Int. J. Numer. Methods Eng., 74 (2008), pp. 1519–1559.

[12] J. A. S. WITTEVEEN, *Explicit and robust inverse distance weighting mesh deformation for CFD,* AIAA 2010-165, January 2010.

[13] L. UYTTERSPROT, Inverse Distance Weighting Mesh Deformation, Master thesis, Delft University of Technology, 2014.

[14] E. LUKE, E. COLLINS AND E. BLADES, *A fast mesh deformation method using explicit interpolation,* J. Comput. Phys., 231(2) (2012), pp. 586–601.

[15] X. ZHOU AND S. X. LI ET AL., *Advances in the research on unstructured mesh deformation,* Adv. Mech., 05 (2011), pp. 547–561.

[16] J. A. S. WITTEVEEN AND H. BIJL, *Explicit mesh deformation using inverse distance weighting interpolation,* AIAA 2009-3996, June 2009.

[17] G. Y. LU AND D. W. WONG, *An adaptive inversedistance weighting spatial interpolation technique,* Comput. Geosci., 34(9) (2008), pp. 1044–1055.

[18] D. SHEPARD, *A two-dimensional interpolation function for irregularly-spaced data,* Proceedings of the 1968 23rd ACM National Conference, pages 517–524, 1968.

[19] L. DING, T. Q. GUO AND Z. L. LU, *A hybrid method for dynamic mesh generation based on radial basis functions and delaunay graph mapping,* Adv. Appl. Math. Mech., 6(1) (2014), pp. 120–134.

[20] W. T. JONES AND J. SAMAREH-ABOLHASSANI, *A grid generation system for multi-disciplinary design optimization,* AIAA Paper 95-1689, June 1995.

[21] L. DING, Z. L. LU AND T. Q. GUO, *An efficient dynamic mesh generation method for complex multi-block structured grid,* Adv. Appl. Math. Mech., 6(1) (2014), pp. 120–134.

[22] D. J. DALLE AND K. J. FIDKOWSKI, *Multifidelity airfoil shape optimization using adaptive mesh-*

https://doi.org/10.4208/aamm.2016.m1423 Published online by Cambridge University Press

ing, AIAA Paper 2014-2996, June 2014.
[23] T. NAMBU, D. J. MAVRIPLIS AND K. MANI, *Adjoint-based shape optimization of high-lift airfoils using the NSU2D unstructured mesh solver*, AIAA Paper 2014-0554, January 2014.
[24] AGARD Report, Compendium of Unsteady Aerodynamic Measurements, AGARD Report No. 702, 1983.
[25] J. LI AND S. Z. HUANG ET AL., *Unsteady viscous flow simulations by a fully implicit method with deforming grid*, AIAA Paper 2005-1221, January 2005.

https://doi.org/10.4208/aamm.2016.m1423 Published online by Cambridge University Press